The near-infrared to ultraviolet continuum of radio-loud versus radio-quiet quasars

M. Labita,[1★] A. Treves[1] and R. Falomo[2]
[1]Department of Physics and Mathematics, University of Insubria, Via Valleggio 11, I-22100 Como, Italy
[2]INAF, Astronomical Observatory of Padova, Vicolo dell'Osservatorio 5, I-35122 Padova, Italy

Accepted 2007 October 27. Received 2007 October 23; in original form 2007 July 10

ABSTRACT

Starting from a sample of Sloan Digital Sky Survey quasars appearing also in the Two-Micron All-Sky Survey, we study the continuum properties of ∼1000 objects observed in eight bands, from near-infrared to ultraviolet. We construct the mean spectral energy distribution (SED) and compare and contrast the continua of radio-loud and radio-quiet quasar (RLQ and RQQ, respectively) objects. The SEDs of the two populations are significantly different, in the sense that RLQs are redder with power-law spectral indices $\langle\alpha_{\rm RLQ}\rangle = -0.55 \pm 0.04$ and $\langle\alpha_{\rm RQQ}\rangle = -0.31 \pm 0.01$ in the spectral range between $10^{14.5}$ and $10^{15.35}$ Hz. This difference is discussed in terms of different extinctions, different disc temperatures, or slopes of the non-thermal component.

Key words: galaxies: active – galaxies: nuclei – quasars: general.

1 INTRODUCTION

A substantial effort has been dedicated to construct the spectral energy distributions (SEDs) for sizeable samples of quasars over the whole accessible range of the electromagnetic spectrum (see e.g. Sanders et al. 1989; Francis et al. 1991; Elvis et al. 1994; Richards et al. 2006). However, only a few papers focus on the comparison between the SEDs of radio-loud and radio-quiet quasars (RLQs and RQQs, respectively). Elvis et al. (1994) propose an overall spectrum from a sample of 47 quasars, divided in RLQs and RQQs, which shows that no distinction between the SEDs of the two subsamples is apparent in the range $100\mu - 1000$ Å. As noted by these authors, the considered sample is biased towards X-ray and optically bright quasars. Some indication of a possible difference between the near-infrared (NIR) to optical colours of RLQs and RQQs in the Two-Micron All-Sky Survey (2MASS) catalogue was reported by Barkhouse & Hall (2001). Francis, Whiying & Webster (2000) found that the optical–NIR continuum is significantly redder in radio-selected RLQs from the PKS Half-Jansky Flat-Spectrum survey than in optically selected RQQs from the Large Bright Quasar Survey (LBQS). These and other works (e.g. Kotilainen et al. 2007) indicate that RLQ objects are possibly redder than their radio-quiet counterparts, but the samples seriously suffer from selection effects against red RQQs, because RQQs are mostly collected from optically selected samples (e.g. the LBQS, the first selection criterion of which is the 'blue colour' of candidates; see Hooper, Impey & Foltz 1997). White et al. suggest that redder quasars from the Sloan Digital Sky Survey (SDSS) are likely to be more radio powerful than bluer objects, and this is an indication that the red colour of RLQ objects is not completely due to the bias against red RQQs in optically selected samples, since the two classes of objects derive from the same survey.

Because of the importance of the distinction between RLQs and RQQs in the Unified Models of active galactic nuclei, these results suggest and motivate a study aimed at investigating the properties of the continuum emission of quasars in the ultraviolet (UV) to NIR region, in order to compare and contrast the SEDs of RLQ and RQQ objects.

In Section 2, we focus on the quasar sample selection criteria and on the host galaxy contribution. In Section 3, we consider the SED construction and discuss the spectral shape. The RLQ and RQQ SEDs are then compared and contrasted. In the last section, we provide a summary and a discussion of the results.

Throughout this paper, we adopt a concordant cosmology with $H_0 = 70\,{\rm km\,s^{-1}\,Mpc^{-1}}$, $\Omega_{\rm m} = 0.3$ and $\Omega_\Lambda = 0.7$.

2 SAMPLE SELECTION

In order to mark similarities and differences of the continuum spectroscopic properties of RLQs and RQQs, our first aim is the selection of a quasar sample which is minimally biassed against the radio properties and the nuclear colour of the objects. We start our analysis from the SDSS quasar catalogue III (Schneider et al. 2005); we then require that objects are in the observation area of the Faint Images of the Radio Sky at Twenty-cm (FIRST, Becker et al. 2003), which is the reference catalogue for radio data, in order to allow the distinction between RLQs and RQQs. Finally, this sample is cross-correlated with the Two-Micron All-Sky Survey (2MASS, Cutri et al. 2003) in order to have detections in the NIR bands.

★E-mail: marzia.labita@uninsubria.it

Table 1. Extract from the final sample. Monochromatic fluxes are derived from SDSS (columns 4–8), 2MASS (columns 9–11) and FIRST (column 12) and corrected for Galactic extinction; units are 10^{-4} Jy. In column (12), 'n.d.' means 'not detected'. The complete version of this table is available as Supplementary Material to the electronic version of this article on Blackwell Synergy.

					SDSS				2MASS		FIRST	
α (J2000) (1)	δ (J2000) (2)	z (3)	F_u (4)	F_g (5)	F_r (6)	F_i (7)	F_z (8)	F_J (9)	F_H (10)	F_K (11)	$F_{20\,\mathrm{cm}}$ (12)	$R_{\mathrm{r-o}}$ (13)
00 01 10.97	−10 52 47.5	0.528	2.69	3.40	3.21	3.53	3.24	3.38	4.82	6.46	n.d.	<10
00 14 20.37	−09 18 49.4	1.083	2.01	2.82	4.25	3.95	3.97	5.26	4.12	6.80	57.3	19.6
00 18 55.22	−09 13 51.2	0.756	2.86	4.25	5.09	5.12	5.62	5.88	6.07	7.12	n.d.	<10
00 24 11.66	−00 43 48.1	1.795	1.73	2.08	2.29	2.69	2.57	2.67	3.44	4.88	11.7	5.55
00 29 14.21	−09 00 16.1	2.091	0.71	1.16	1.66	2.02	2.70	3.60	3.46	5.37	n.d.	<10
00 30 09.40	−09 02 23.1	1.786	2.59	2.51	2.69	3.42	3.41	3.09	5.26	3.25	n.d.	<10
00 34 13.04	−01 00 26.9	1.292	4.72	5.03	5.64	5.81	5.54	5.08	5.62	6.86	n.d.	<10
00 36 26.11	−09 00 14.2	0.951	1.86	1.93	2.05	1.89	1.89	2.88	1.83	4.98	n.d.	<10
00 36 33.93	−10 12 28.8	2.082	1.63	1.89	2.06	2.33	2.68	2.69	2.79	4.05	n.d.	<10
00 37 14.82	−00 45 54.1	1.020	1.66	1.86	2.12	1.96	2.16	2.48	1.65	3.41	n.d.	<10
00 38 23.81	−00 00 25.1	1.605	1.63	1.79	2.12	2.52	2.67	3.33	3.12	3.11	n.d.	<10
00 38 42.66	−09 47 12.8	1.989	3.65	3.97	4.45	4.82	5.29	4.39	3.60	5.18	n.d.	<10
00 42 22.29	−10 37 43.8	0.424	9.13	11.3	9.75	10.0	12.5	7.87	10.8	17.8	n.d.	<10
00 46 13.54	+01 04 25.7	2.152	1.51	1.90	2.27	2.70	3.11	4.02	4.41	6.35	30.4	15.6
...	...	...	...	...	...	...	...	...	...	...	...	...

2.1 SDSS quasar catalogue

The SDSS quasar catalogue (46 420 objects) covers about 4188 deg^2 and selects objects that have luminosities larger than $M_i = -22$, have at least one emission line with full width at half-maximum larger than 1000 km s^{-1} or are unambiguously broad absorption-line objects, are fainter than $i = 15.0$ and have highly reliable redshifts.

Note that the SDSS quasar catalogue suffers from a small bias in favour of RLQ objects, as a FIRST detection is one of the starting criteria to select quasar candidates; anyway White et al. (2007) verified that this introduces at most a very minor bias towards higher radio–optical ratios.

2.2 FIRST: distinction between RLQs and RQQs

Starting from the SDSS quasars, we focus on those which are in the FIRST observation area, but we do not exclude a priori the objects which are under the FIRST flux limit (1 mJy), so that no bias against the radio power is introduced. The distinction between RLQ and RQQ objects is usually made referring to the ratio between the radio and optical flux. Here, we assume that a quasi-stellar object (QSO) is radio loud if

$$R_{\mathrm{r-o}} = \frac{F_\nu(1.5 \times 10^9\ \mathrm{Hz})}{F_\nu(6 \times 10^{14}\ \mathrm{Hz})} > 10 \qquad (1)$$

and radio quiet otherwise[1] (e.g. Kellermann et al. 1989). Note that our division between RLQs and RQQs should not be considered a physical bimodality, an issue on which there is still controversy in the literature (e.g. Goldschmidt et al. 1999; Ivezić et al. 2002; Jiang et al. 2007). Yet our division is a simple separation in two groups of high or low radio power with respect to a certain limit. We verified that all the results presented here remain substantially unchanged adopting different limits (5 or 30) for the distinction between RLQ and RQQ objects.

There are not radio data for all the objects in the sample (91 per cent of the objects are below the FIRST radio flux limit), and obviously the larger part of these are expected to be RQQ objects. In order not to introduce a bias against the ratio of RLQs and RQQs, we select all the objects which have $g < 18.9$, so that for this subsample we can discriminate between RLQs and RQQs. In fact, if an object has a radio flux under the FIRST limit [i.e. $F_\nu(1.5 \times 10^9\ \mathrm{Hz}) < 1$ mJy] and $g < 18.9$ [i.e. $F_\nu(6 \times 10^{14}\ \mathrm{Hz}) > 0.1$ mJy], because of condition (1) it is an RQQ, while we could not discriminate if $g > 18.9$. This restriction reduces the sample by 66 per cent, keeping the original ratio between the number of RQQs and RLQs. We obtain a sample of 14 395 objects, 1105 of which are RLQs and 13 290 are RQQs . From the SLOAN data, we derived the u, g, r, i, z magnitudes. The values were corrected for Galactic extinction, following the indications given in Schneider et al. (2005).

2.3 NIR detections from 2MASS

The SLOAN–FIRST sample was then cross-correlated with the 2MASS catalogue, in order to obtain the J, H and K magnitudes of the objects. The 2MASS survey is a collection of NIR uniformly calibrated observations of the entire sky; sources brighter than about 1 mJy in each band were detected with a signal-to-noise ratio greater than 10. The cross-correlation strongly reduces the sample, which now consists of 1761 common objects with observations in eight bands each. We assumed that two objects are matched if their separation angle is less than 0.2 arcsec, which roughly corresponds to the position error of the catalogues.[2] Obviously, the request of a 2MASS detection introduces a bias in the sample, as among high-redshift (low-luminosity) objects the redder ones are more likely detected. In the following, we will come back to this issue.

[1] Equation (1) should be applied to rest-frame data, but this correction requires the assumption of a spectral shape of the objects. Here, we choose to evaluate this ratio based on observed data; we verified that the difference is completely negligible.

[2] We verified that this limit on the separation angle causes the omission of about 20 per cent of objects which belong to both catalogues, but drastically reduces the probability of mismatch in the selection of the objects.

2.4 Host galaxy component

A host galaxy component could affect the luminosity measures in part of the selected quasars. We require the selected objects to have a negligible galaxy component with respect to the nuclear flux. Assuming that all the galaxies are ellipticals (SED from Mannucci et al. 2001), purely passively evolving (Bressan, Chiosi & Fagotto 1994), with $M_R = -22.6$ for RLQs and $M_R = -21.8$ for RQQs at $z \sim 0$ (see e.g. Kotilainen et al. 2007), we give a first-order estimate of the galaxy component flux in the eight SLOAN and 2MASS filters. An object is excluded from the sample if the estimated flux of the host galaxy is greater than 20 per cent of the observed flux. The excluded objects ($\sim$1000) are mostly weak, nearby ($z < 0.5$) quasars. We also tested if the removal of quasars with substantial host galaxies could be done by looking at the difference between point spread function and model magnitudes in SDSS. The results reported in the following remain substantially unchanged.

2.5 Final sample

The final sample (see Table 1) consists of 887 QSOs, of which 774 are RQQs and the rest RLQs.

Figs 1 and 2 show the magnitude and redshift distributions of the RLQ and RQQ subsamples, indicating a substantial difference between the two classes. This behaviour is well known and it is usually attributed to the cosmological evolution of quasar radio properties or to a different density evolution for RLQs and RQQs (e.g. White et al. 2007; Jiang et al. 2007). The issue is obviously relevant to our discussion and it is considered in Section 3.

3 SPECTRAL ENERGY DISTRIBUTIONS

In order to construct and compare the SEDs of RQQs and RLQs, we first evaluated the rest-frame SEDs of single objects. For each one, the SED consists of eight data points $\log(\nu)$– $\log(\nu L_\nu)$, which are linearly interpolated. In order not to be affected by the well-known bias which favours more luminous objects at higher redshift, using the standard procedure (e.g. Elvis et al. 1994), the SEDs of the RLQ and RQQ samples have then been normalized separately at $10^{14.8}$ Hz.

The average SEDs of the two samples have been determined evaluating the average value of $\log(\nu L_\nu)$ at each frequency.

Fig. 3 shows the mean SED of the whole sample and those of the RLQ and RQQ subsamples, and in Table 2 we give the number

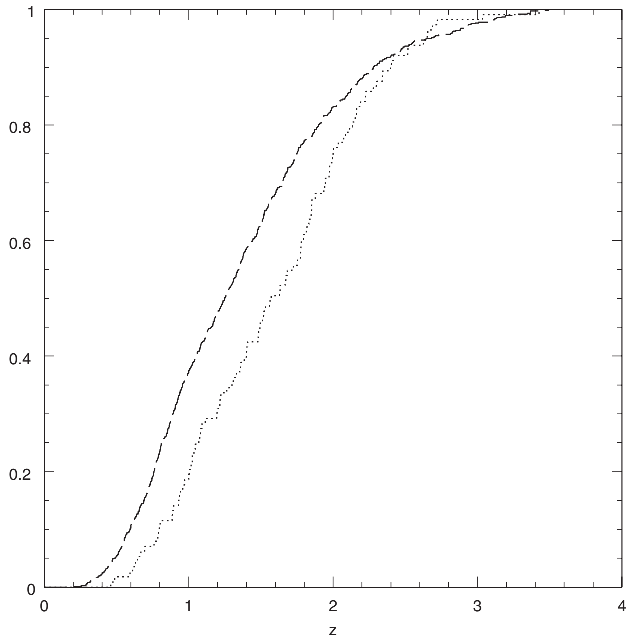

Figure 1. Cumulative redshift distribution of the final sample. The dotted line refers to the RLQs and the dashed line to the RQQs.

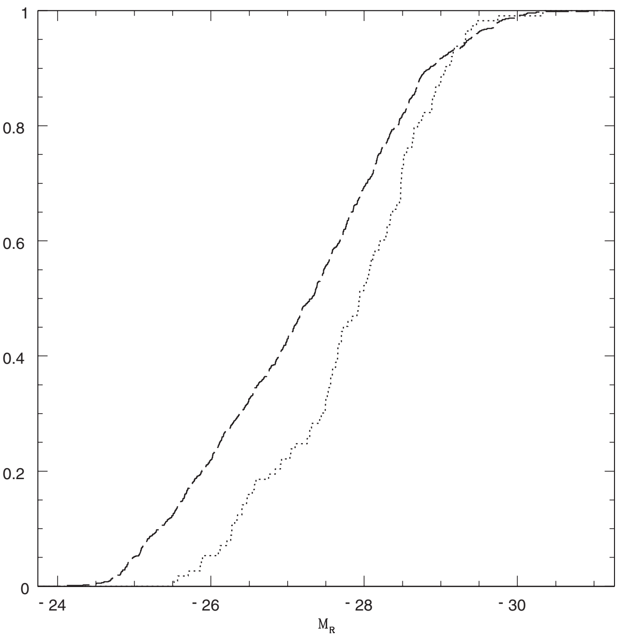

Figure 2. Cumulative M_R distribution of the final sample. The dotted line refers to the RLQs and the dashed line to the RQQs.

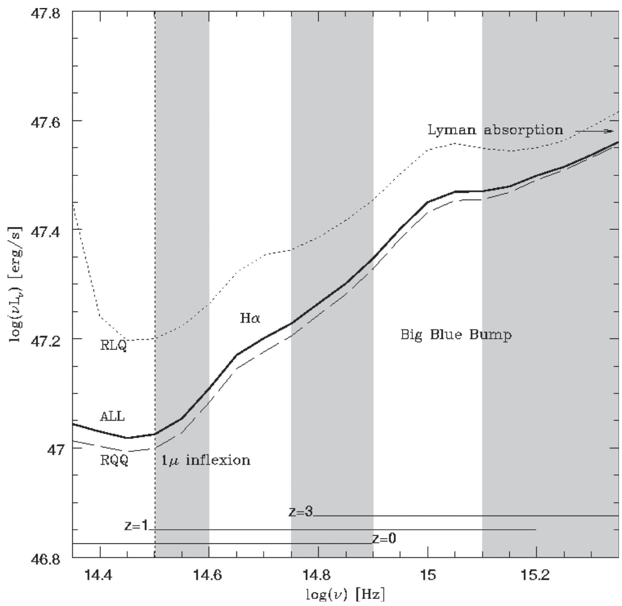

Figure 3. SED for the entire sample of quasar (solid line), RLQs (dotted line) and RQQs (dashed line). The horizontal lines show the spectral region available at different redshifts. The grey regions indicate the spectral ranges where the power-law fit is performed.

Table 2. For selected frequencies, we report the number of data points which contribute to the SED of RLQs and RQQs, the mean redshift and its standard deviation, the luminosity, its standard deviation and the error on the mean. The luminosities are normalized at $\log(\nu L_\nu(10^{14.8}\ \mathrm{Hz}))$.

	RLQ			RQQ		
$\log(\nu)$ (Hz)	Number	z	$\log(\nu L_\nu)$ (erg s^{-1})	Number	z	$\log(\nu L_\nu)$ (erg s^{-1})
14.35	3	0.514 ± 0.070	47.446 ± 0.292 (±0.207)	87	0.481 ± 0.098	47.013 ± 0.132 (±0.014)
14.40	13	0.671 ± 0.115	47.241 ± 0.163 (±0.047)	190	0.613 ± 0.145	47.003 ± 0.123 (±0.009)
14.45	26	0.815 ± 0.171	47.197 ± 0.172 (±0.034)	301	0.725 ± 0.190	46.993 ± 0.117 (±0.007)
14.50	39	0.924 ± 0.213	47.200 ± 0.145 (±0.023)	398	0.829 ± 0.250	46.999 ± 0.105 (±0.005)
14.55	55	1.069 ± 0.293	47.223 ± 0.131 (±0.018)	513	0.961 ± 0.331	47.028 ± 0.102 (±0.004)
14.60	76	1.256 ± 0.396	47.264 ± 0.115 (±0.013)	609	1.077 ± 0.407	47.084 ± 0.097 (±0.004)
14.65	95	1.412 ± 0.475	47.321 ± 0.091 (±0.009)	686	1.184 ± 0.489	47.145 ± 0.089 (±0.003)
14.70	106	1.511 ± 0.536	47.353 ± 0.072 (±0.007)	733	1.261 ± 0.559	47.176 ± 0.074 (±0.003)
14.75	112	1.576 ± 0.591	47.363 ± 0.040 (±0.004)	757	1.311 ± 0.615	47.205 ± 0.039 (±0.001)
14.80	113	1.592 ± 0.613	47.386 ± 0.000 (±0.000)	774	1.353 ± 0.671	47.244 ± 0.000 (±0.000)
14.85	113	1.592 ± 0.613	47.417 ± 0.036 (±0.003)	774	1.353 ± 0.671	47.281 ± 0.030 (±0.001)
14.90	113	1.592 ± 0.613	47.454 ± 0.067 (±0.006)	774	1.353 ± 0.671	47.328 ± 0.051 (±0.002)
14.95	113	1.592 ± 0.613	47.502 ± 0.090 (±0.008)	774	1.353 ± 0.671	47.384 ± 0.064 (±0.002)
15.00	113	1.592 ± 0.613	47.546 ± 0.108 (±0.010)	772	1.356 ± 0.669	47.432 ± 0.077 (±0.003)
15.05	113	1.592 ± 0.613	47.558 ± 0.119 (±0.011)	752	1.383 ± 0.657	47.453 ± 0.087 (±0.003)
15.10	110	1.622 ± 0.595	47.549 ± 0.131 (±0.013)	695	1.454 ± 0.633	47.455 ± 0.097 (±0.004)
15.15	103	1.685 ± 0.560	47.544 ± 0.150 (±0.015)	599	1.574 ± 0.600	47.468 ± 0.110 (±0.005)
15.20	90	1.798 ± 0.507	47.550 ± 0.179 (±0.019)	481	1.741 ± 0.553	47.491 ± 0.128 (±0.006)
15.25	75	1.935 ± 0.439	47.563 ± 0.207 (±0.024)	386	1.891 ± 0.515	47.509 ± 0.134 (±0.007)
15.30	59	2.079 ± 0.381	47.589 ± 0.207 (±0.027)	269	2.108 ± 0.472	47.532 ± 0.157 (±0.010)
15.35	41	2.241 ± 0.345	47.616 ± 0.189 (±0.030)	173	2.350 ± 0.422	47.556 ± 0.149 (±0.011)

of data points which contribute to the mean for selected values of $\log(\nu)$, the corresponding average z and the mean value of $\log(\nu L_\nu)$ with corresponding errors. The overall SEDs are similar to those reported by Elvis et al. (1994) and Richards et al. (2006) (see Fig. 4). The strongest feature is the so-called 1-μm inflexion, where the slope of the SED changes sign in a νL_ν versus ν representation. Here, the optical–UV continuum rises above the IR and forms a 'UV bump' (e.g. Shields 1978; Malkan & Sargent 1982; Elvis et al. 1994), which is most often interpreted in terms of thermal emission from an accretion disc (e.g. Malkan 1983; Czerny & Elvis 1987).

At high frequencies ($\nu \gtrsim 10^{15.35}$ Hz), the SEDs of all the objects are strongly contaminated by the Lyman α forest; the small bump at $\sim 10^{14.66}$ Hz is due to the presence of the Hα large emission line.

It is apparent that RLQs are softer than RQQs. In particular, we compare the slope between the 1-μm inflexion and the Lyman α forest. The spectral index α (such that $F_\nu \propto \nu^\alpha$) is derived for each object by fitting with a power law the observed fluxes in the spectral range between $10^{14.5}$ and $10^{15.35}$ Hz, excluding the data points affected by the most-prominent emission features (i.e. $\sim 10^{14.6}$–$10^{14.75}$ Hz, $10^{14.9}$–$10^{15.1}$ Hz).

Table 3 reports the mean values of α, the standard deviation and the error on the mean value for the RLQ and RQQ subsamples and Fig. 5 shows the cumulative distribution of the spectral index for the two populations. The slopes of the RLQs and RQQs are statistically different at more than 99 per cent confidence level, with RLQs being softer. The spectral indices of the two populations in the optical region differ by ~ 0.2, with $\alpha = -0.55 \pm 0.41(\pm\ 0.04)$ for RLQs and $\alpha = -0.31 \pm 0.32(\pm\ 0.01)$ for RQQs (where the uncertainties are the standard deviations and the errors on the mean, respectively). A Kolmogorov–Smirnov test indicates that the probability of RLQs and RQQs to be drawn from the same underlying population is negligible ($P \sim 10^{-7}$). This is a strong indication that the two populations are intrinsically different, in the sense that RLQ objects are systematically redder than RQQs.

In Section 2.3, we noted that the request of a 2MASS detection introduces a bias in the sample, as among high-redshift (low-luminosity) objects the redder ones are more likely detected. Consequently, the blue side of the resulting SEDs (which is dominated by high-redshift objects) are slightly softer with respect to the SED of an unbiased sample. This effect can be quantified by constructing the mean SEDs on the whole SLOAN sample, that is, without the request of a 2MASS detection. The shape of the SEDs is modified as expected by the bias introduced, but it is notable that the difference between the SEDs of RLQs and RQQs (which is our main result) remains substantially unchanged if we consider the whole SLOAN sample to construct the SED for $\log(\nu) > 14.8$ (where the 2MASS data are not relevant) and the SLOAN–2MASS sample to construct the SED for $\log(\nu) < 14.8$ (where the introduced bias is negligible). The average spectral indices of the RLQ and RQQ populations, as determined on these SEDs, are, respectively, $\alpha = -0.40$ and -0.22, with again $\Delta\alpha \sim 0.2$.

Since we are interested in the study of the shape of the SED with reference to the radio power, independently of any other parameter, we now construct a number of RQQ samples matched in absolute magnitude to the RLQs.[3] We verify that the RQQ matched samples automatically result well matched to the RLQs also in redshift.

Table 3 reports the average results of 10 random matched samples. The SEDs of the RQQ matched samples are on average slightly softer than those of the entire RQQ population ($\Delta\alpha = 0.05$); however, the Kolmogorov–Smirnov test indicates that the probability of RLQs and all the RQQ matched samples to be drawn from the

[3] An RQQ with a given luminosity L is extracted from the RQQ population with probability proportional to the luminosity density of the RLQs.

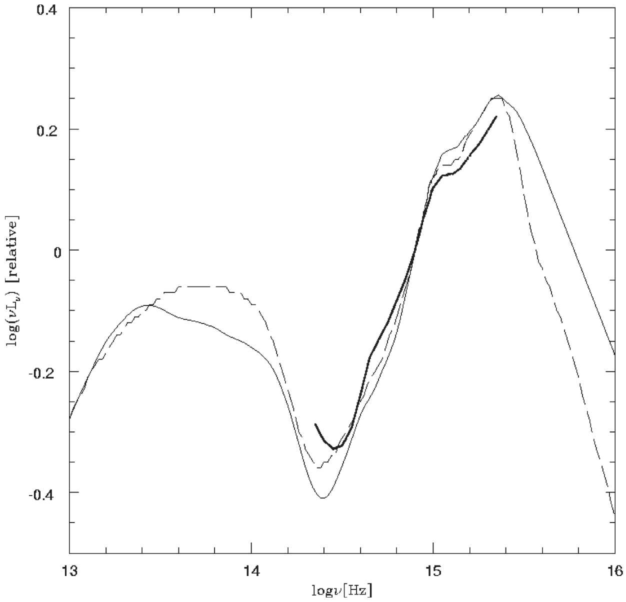

Figure 4. SED for our entire sample of quasars (thick solid line), compared to the SEDs obtained by Elvis et al. (1994) (thin solid line) and by Richards et al. (2006) (thin dashed line). The three SEDs have been normalized at $10^{14.9}$ Hz.

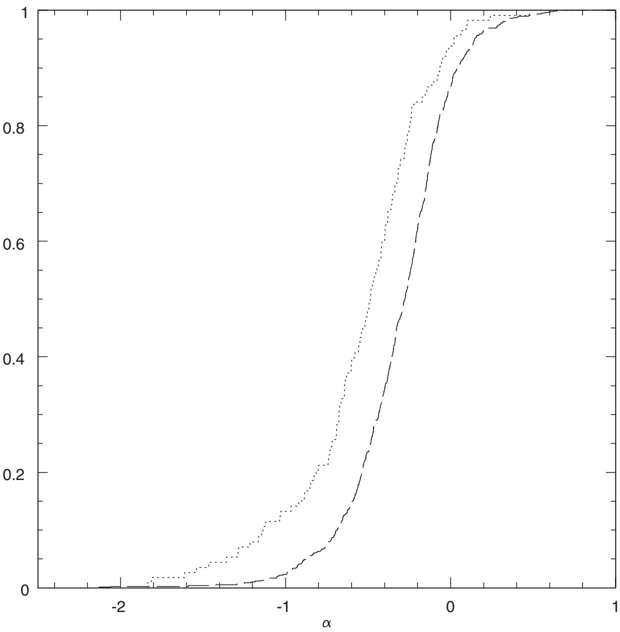

Figure 5. Cumulative distribution of the spectral index for the RLQ (dotted line) and RQQ (dashed line) subsamples.

same underlying population is still negligible ($P \sim 10^{-3}$; the value is greater than before as the sample has been drastically reduced), and the difference of the mean spectral indices is again ∼0.2. This is consistent with the fact that the whole RQQ population and an RQQ matched sample have identical distributions in α ($P \sim 90$ per cent) and it is a strong indication that the RLQ and RQQ populations are intrinsically different, in the sense that RLQ objects are systematically redder than RQQs independently of the average luminosity or cosmic time.

Finally, we compare RLQs and RQQs in different redshift bins (see again Table 3), and this test shows that the colour difference between the RLQ and RQQ populations is apparent in all the redshift ranges.

4 SUMMARY AND DISCUSSION

The aim of this paper is the study of the continuum emission in the NIR to UV region of a quasar sample, in order to compare and contrast the SEDs of the RLQ and RQQ subsamples. We selected a sample of quasars with both SLOAN and 2MASS detection, to study a spectral range from the NIR (for low-z objects) to the UV (for high-z QSOs). The sample consists of 887 objects, of which 113 are RLQs and the rest are RQQs.

For each subsample, we constructed the mean SED and evaluated the average spectral index in the NIR to UV region. The slope of the underlying power laws is significantly different: the spectral indices of the two populations are statistically different at more than 99 per cent confidence, both for the whole sample and dividing the sample in redshift bins. The difference is present also considering samples well matched in absolute magnitude and redshift.

If the blue bump is due to the superposition of blackbody emission from an accretion disc, then the colour difference between RLQs and RQQs should be interpreted in terms of different mean temperatures, in the sense that RQQs are hotter.

We first examine the possibility that the difference in the SEDs of RLQs and RQQs is due to an enhanced dust extinction in RLQ objects, as it has been suggested, for example, by Francis et al. (2000). In Fig. 6, we compare the SED of RQQs to the SED of RLQs, when RLQs are additionally corrected for dust extinction with respect to RQQs: the offset between the SEDs of the two populations is minimized by adopting $\Delta A_V = 0.16$ mag. The differences are now

Table 3. Mean values of the spectral index α in the optical–UV region, standard deviation and error on the mean, for the RLQ and RQQ subsamples. Column (6) reports the Kolmogorov–Smirnov probability that the RLQs and the RQQs (or RQQ matched sample) are drawn from the same population.

Samples (1)	# RLQ (2)	α_{RLQ} (3)	# RQQ (4)	α_{RQQ} (5)	P_{KS} (6)
Total sample	113	$-0.55 \pm 0.41(\pm0.04)$	774	$-0.31 \pm 0.32(\pm0.01)$	10^{-7}
Matched samples	″	″	112	$-0.36 \pm 0.29(\pm0.03)$	10^{-3}
$z < 0.8$	12	$-0.64 \pm 0.55(\pm0.16)$	181	$-0.21 \pm 0.37(\pm0.03)$	10^{-2}
$0.8 < z < 1.2$	23	$-0.41 \pm 0.34(\pm0.07)$	188	$-0.26 \pm 0.31(\pm0.02)$	10^{-1}
$1.2 < z < 1.6$	22	$-0.66 \pm 0.50(\pm0.11)$	157	$-0.34 \pm 0.30(\pm0.02)$	10^{-4}
$1.6 < z < 2.0$	28	$-0.56 \pm 0.40(\pm0.08)$	117	$-0.37 \pm 0.27(\pm0.03)$	10^{-2}
$z > 2.0$	28	$-0.51 \pm 0.34(\pm0.07)$	131	$-0.42 \pm 0.28(\pm0.02)$	10^{-1}

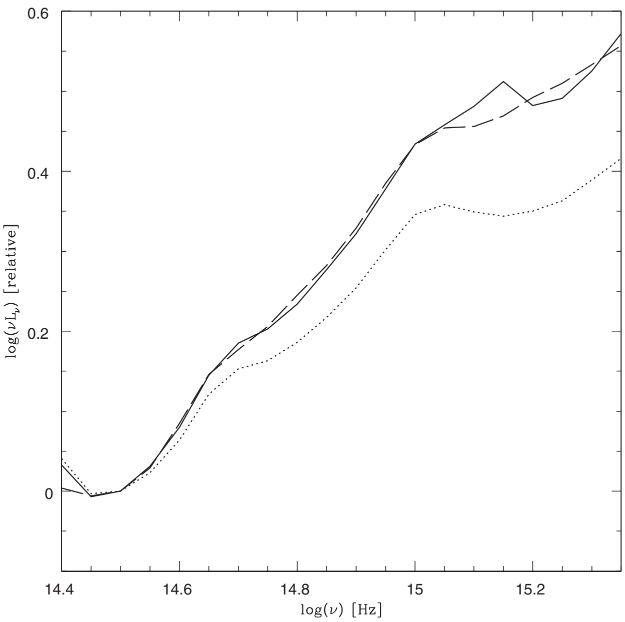

Figure 6. Comparison of the SED of RQQs (dashed line) to the SED of RLQs (dotted line). When RLQs are corrected for an additional dust extinction ($\Delta A_V = 0.16$ mag, solid line), no difference is apparent.

completely negligible, supporting the hypothesis that RLQ objects are more subjected to dust extinction than RQQs. The problem would be reconducted to understand why RLQs are more extincted than RQQs. A priori this could be related to a difference in the inclination angle distribution. Alternatively, it could be that the conditions of dust production are related to those justifying large radio emission.

We then focus on the possibility that the difference in disc temperatures of RLQs and RQQs is real. Since the temperature of the inner disc scales as $M_{\rm BH}^{-0.25}$ (e.g. Shakura & Sunyaev 1973), the difference may be attributed to the fact that the black holes (BHs) of RLQs are supposedly more massive (e.g. Dunlop et al. 2003; Falomo et al. 2004; Labita, Falomo & Treves 2007).

The colour difference may be linked to the BH spin (Stawarz, Sikora & Lasota 2007), as radio emission is usually ascribed to a faster spinning. However, spinning BHs are expected to have a shorter last stable orbit radius, and then a hotter disc, inconsistent with our results.

Obviously, it is possible that the non-thermal (power-law) continua of RLQs and RQQs are intrinsically different. Supposing that the non-thermal component accounts for 80 per cent at $10^{14.5}$ Hz, while at $10^{15.35}$ Hz (in the Big Blue Bump) the thermal component is dominant and accounts for 80 per cent, our data are consistent with a picture where the underlying power laws of RLQs and RQQs have $\alpha_{\rm RLQ} = -1.2$ and $\alpha_{\rm RQQ} = -1.0$, respectively, whereas the thermal bumps are indistinguishable. The problem would be reconducted to understand why the non-thermal continuum of RLQs is softer than that of RQQs. It has been suggested (i.e. Francis et al. 2000) that in RLQ samples there is a significant chance of synchrotron contamination of the rest-frame *R*-band nuclear luminosities, due to the presence of the relativistic jets. This effect explains the red colour of QSOs in high-frequency selected radio samples (i.e. the PKS survey, e.g. Francis et al. 2001), that suffer from a bias towards pole-on radio sources which are relativistically boosted above the survey flux limit, but no obvious explanation can be invoked to justify the colour difference in our sample.

ACKNOWLEDGMENTS

We are grateful to Dr M. Strauss for constructive criticism, and to Dr D. Bettoni for help in the use of SLOAN archives. This work was partially supported by PRIN 2005/32.

REFERENCES

Barkhouse W. A., Hall P. B., 2001, AJ, 121, 284
Becker R. H., Helfand D. J., White R. L., Gregg M. D., Laurent-Muehleisen S. A., 2003, VizieR On-line Data Catalog, VIII/71
Bressan A., Chiosi C., Fagotto F., 1994, ApJS, 94, 63
Cutri R. M. et al., 2003, VizieR On-line Data Catalog, II/246
Czerny B., Elvis M., 1987, ApJ, 321, 305
Dunlop J. S., McLure R. J., Kukula M. J., Baum S. A., O'Dea C. P., Hughes D. H., 2003, MNRAS, 340, 1095
Falomo R., Kotilainen J. K., Pagani C., Scarpa R., Treves A., 2004, ApJ, 604, 495
Elvis M. et al., 1994, ApJS, 95, 1
Francis P. J., Hewett P. C., Foltz C. B., Chaee F. H., Weymann R. J., Morris S. L., 1991, ApJ, 373, 465
Francis P. J., Whiying M. T., Webster R. L., 2000, PASA, 53, 56
Francis P. J., Drake C. L., Whiting M. T., Drinkwater M. J., Webster R. L., 2001, PASA, 18, 221
Goldschmidt P., Kukula M. J., Miller L., Dunlop J. S., 1999, ApJ, 511, 612
Hooper E. J., Impey C. D., Foltz C. B., 1997, ApJ, 480, L95
Ivezić Z. et al., 2002, AJ, 124, 2364
Jiang L., Fan X., Ivezić Z., Richards G. T., Schneider D. P., Strauss M. A., Kelly B. C., 2007, ApJ, 656, 680
Kellermann K. I., Sramek R., Schmidt M., Shaffer D. B., Green R., 1989, AJ, 98, 1195
Kotilainen J. K., Falomo R., Labita M., Treves A., Uslenghi M., 2007, ApJ, 660, 1039
Labita M., Falomo R., Treves A., 2007, MNRAS, 373, 551
Malkan M. A., 1983, ApJ, 268, 582
Malkan M. A., Sargent W. L. W., 1982, ApJ, 254, 22
Mannucci F., Basile F., Poggianti B. M., Cimatti A., Daddi E., Pozzetti L., Vanzi L., 2001, MNRAS, 326, 745
Richards G. T. et al., 2006, ApJS, 166, 470
Sanders D. B., Phinney E. S., Neugebauer G., Soifer B. T., Matthews K., 1989, ApJ, 347, 29
Schneider et al., 2005, AJ, 130, 367, VizieR On-line Data Catalog, VII/243
Shakura N. I., Sunyaev R. A., 1973, A&A, 24, 337
Shields G. A., 1978, Nat, 272, 706
Stawarz L., Sikora M., Lasota J. P., 2007, in Rector T. A., De Young D. S., eds, ASP Conf. Ser., Extragalactic Jets: Theory and Observation from Radio to Gamma Ray. San Francisco, preprint (astro-ph/0707.2369)
White R. L., Helfand D. J., Becker R. H., Glickman E., de Vries W., 2007, ApJ, 654, 99

This paper has been typeset from a TEX/LATEX file prepared by the author.